GRO J0422+32: THE LOWEST MASS BLACK HOLE?[1]

DAWN M. GELINO

Center for Astrophysics and Space Sciences, Mail Code 0424, 9500 Gilman Drive, University of California at San Diego,
La Jolla, CA 92093-0424; dgelino@ucsd.edu

AND

THOMAS E. HARRISON

Department of Astronomy, New Mexico State University, Box 30001, MSC 4500, Las Cruces, NM 88003-8001;
tharriso@nmsu.edu

ABSTRACT

We have obtained optical and infrared photometry of the soft X-ray transient GRO J0422+32. From this photometry, we find a secondary star spectral type of M1, and an extinction of $A_V = 0.74 \pm 0.09$. We present the first observed infrared (J-, H-, and K-band) ellipsoidal variations, and model them with WD98, a recent version of the Wilson-Devinney light curve–modeling code. Assuming no significant contamination of the infrared light curves, we find a lower limit to the inclination angle of $43°$ corresponding to an upper limit on the mass of the compact object of 4.92 $M_\odot$. Combining the models with the observed spectral energy distribution of the system, the most likely value for the orbital inclination angle is $45° \pm 2°$. This inclination angle corresponds to a primary black hole mass of 3.97 ± 0.95 $M_\odot$. Thus, we contend that J0422+32 contains the lowest mass stellar black hole reported, and the first to have a measured mass that falls in the 3–5 $M_\odot$ range.

Subject headings: binaries: close — infrared: stars — stars: individual (GRO J0422+32) —
stars: variables: other — X-rays: binaries

1. INTRODUCTION

Soft X-ray transients (SXTs) are a subset of low-mass X-ray binaries that exhibit large and abrupt X-ray and optical outbursts separated by long intervals of quiescence. In most cases the compact object is a black hole and the companion star is a low-mass K- or M-type dwarf (see Charles 2001 for a review). During their periods of quiescence, SXTs are very faint at X-ray and optical wavelengths. However, in this state the secondary stars can dominate the system luminosity and allow us to derive the parameters of the SXT binary.

J0422+32 ($\alpha_{J2000} = 04^h21^m42.8^s$, $\delta_{J2000} = 32°54'26''.6$) was discovered by the Burst and Transient Source Experiment (BATSE) on the Compton Gamma Ray Observatory (CGRO) on 1992 August 5 (Paciesas & Briggs 1992), while the $V \sim 13$ optical counterpart was identified by Castro-Tirado et al. (1993). Since its initial outburst, J0422+32 has been studied by Filippenko, Matheson, & Ho (1995), Beekman et al. (1997), Harlaftis et al. (1999), Webb et al. (2000), and references therein. These authors have found an orbital period of 5.092 hr, a secondary star spectral type of M2±2, a mass ratio of $0.116^{+0.079}_{-0.071}$, and secondary star radial velocity semiamplitude of 372 ± 10 km s^{-1}. The implied mass function for J0422+32 is 1.13 ± 0.09 $M_\odot$ (Harlaftis et al. 1999), well below that of the accepted maximum mass of a neutron star (~ 3.2 $M_\odot$).

The X-ray and optical outburst light curves of J0422+32 resemble those of the SXT prototype, V616 Mon (King, Harrison, & McNamara 1996); however, the source has exhibited recurring optical and X-ray mini-outburst behavior

since 1992, reminiscent of X-ray binaries with neutron star primaries (although J0422+32 is not alone in this respect). In order to determine the nature of the primary object in J0422+32, its mass, and therefore orbital inclination angle, must be accurately measured. As discussed in Gelino, Harrison, & McNamara (2001, hereafter GHM01) and Gelino, Harrison, & Orosz (2001, hereafter GHO01), the best way to find the inclination angle in a noneclipsing system is to model its infrared ellipsoidal light curves. Previously, the only ellipsoidal variations detected from J0422+32 have been in the optical (Callanan et al. 1996; Chevalier & Ilovaisky 1996; Casares et al. 1995; Orosz & Bailyn 1995). One previously published attempt was made to observe the variations in the infrared, where there is a smaller chance of contamination from other sources of light in the system, but even after combining the H- and K-band data, no ellipsoidal variations were seen (Beekman et al. 1997). Nonetheless, orbital inclination angle estimates have still been made. These previously published inclination angles for J0422+32 range from $10°$ (lower limit from Beekman et al. 1997) to $51°$ (upper limit from Filippenko et al. 1995), and correspond to primary masses of 34.8 and 2.4 $M_\odot$, respectively. In addition, Bonnet-Bidaud & Mouchet (1995) compared the intrinsic optical emission line widths of J0422+32 to those of V616 Mon and found that the J0422+32 primary is a neutron star with $M_1 \leq 2.2$ $M_\odot$.

In order to determine the mass, and therefore the nature, of the compact object in J0422+32, we have obtained J-, H-, and K-band light curves and model them here with WD98, a recent version of the Wilson-Devinney light-curve modeling code. In § 2 we describe our observations and data reduction process, and present the infrared photometric light curves. We describe our choices for the relevant WD98 input parameters and present our models of the variations in § 3. Finally, in § 4, based on the presented models, we discuss the nature of the compact object in J0422+32.

2. OBSERVATIONS AND DATA REDUCTION

J0422+32 was observed using GRIM II[2] on the Astrophysical Research Consortium 3.5 m telescope at Apache Point Observatory on 2000 January 23, 24, 25, and 26. The *J*-band data were obtained on all of these nights, while *K$_s$*-band data were obtained only on 2000 January 25 and 26. The data were linearized before averaging the images at one position and subtracting them from the average of the images at the other position. The images were flat-fielded with a dome flat using the usual IRAF[3] packages.

The SXT was observed again on 2003 February 7 and 8 using the Gemini Twin-Arrays Infrared Camera[4] on the Shane 3 m telescope at Lick Observatory. Simultaneous *J*- and *K'*-, and *H*- and *K'*-band data were obtained. The number of counts in each exposure was kept in the linear regime of each chip, as there is no linearization correction available. These data were reduced in the same manner as above using twilight flats.

Aperture photometry was performed on J0422+32 and five nearby field stars. Using the IRAF PHOT package, a differential light curve for each band was generated separately for the 2000 and 2003 data sets, with each point being the average of four beam-switched images. The differential photometric results show that over the course of our observations, the comparison stars did not vary more than expected from photon statistics. Variations were observed in both the 2000 and 2003 data sets. Figure 1 compares the 2000 and 2003 light curves.

As Figure 1 shows, the 2000 and 2003 observations revealed light-curve shapes, amplitudes, and brightnesses that were consistent with each other. This enabled us to combine the two data sets. The final *J*, *H*, and *K$_s$* differential light curves of J0422+32, phased to the ephemeris of Webb et al. (2000), are presented in Figure 2. These light curves represent the first detections of infrared ellipsoidal variations from this SXT.

Optical observations of J0422+32 were obtained with SPIcam[5] on 2001 December 18. The *B*-, *V*-, *R*-, and *I*-band exposures were bias-corrected and flat-fielded before aperture photometry was performed. Standards were also observed to transform these data to the system of Landolt. The colors of J0422+32 can be found in Table 1, along with other quiescent optical and infrared colors published for this SXT.

3. INFRARED LIGHT-CURVE MODELING

The J0422+32 infrared light curves presented in Figure 2 were modeled with WD98 in order to find the orbital inclination angle of the system. Many of the parameters needed for light-curve modeling are based on the nature of the secondary star. Before we can model the infrared light curves of J0422+32, we must first derive the input model parameters, and we do so here.
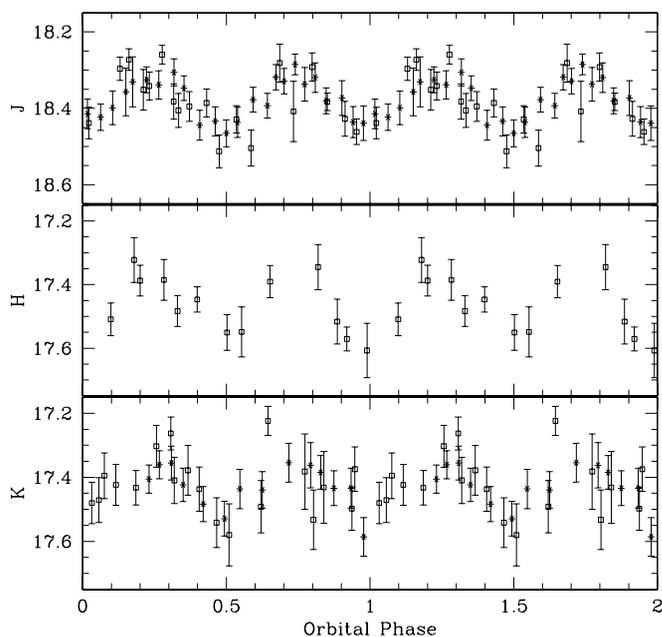
FIG. 1.—Long-term infrared light curves of J0422+32. The *J*- and *K*-band data span 37 months. The asterisks represent data taken 2000 January with the Astrophysical Research Consortium 3.5 m telescope, and the open squares represent data taken 2003 February with the Lick Observatory Shane 3 m telescope. Error bars are 1 σ. These data are plotted over two phase cycles for clarity. Here, and throughout this paper, we phase the J0422+32 heliocentric-corrected data to the ephemeris of Webb et al. (2000). There are no obvious long-term variations in the shapes or mean magnitudes of the light curves.

3.1. *The Nature of the Secondary Star in J0422+32*

The most important parameter for modeling the infrared light curves of any noneclipsing system is the spectral type of the secondary star. This property can be estimated by
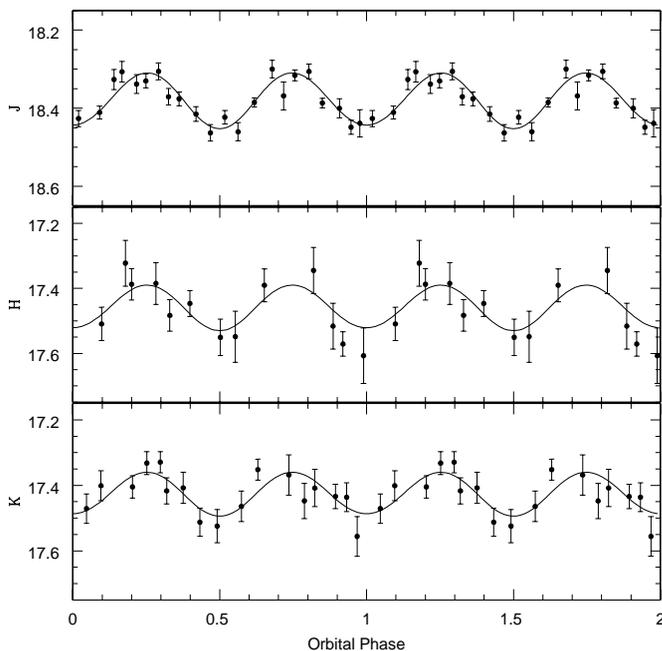

FIG. 2.—J0422+32 *J*-, *H*-, and *K*-band final light curves (*filled circles*). Error bars are 1 σ. The solid line represents the best-fitting ($i = 45°$) WD98 model as described in the text.

TABLE 1
QUIESCENT INFRARED AND OPTICAL COLORS OF J0422+32

Reference	V	$V-R$	$V-I$	K	$J-K$	$H-K$	Date[a]
1..........................	22.39 ± 0.27	1.33 ± 0.29	...	...	...	...	1993 Sep
2..........................	22.24 ± 0.14	1.27 ± 0.17	2.02 ± 0.16	...	...	...	1994 Dec
3..........................	...	...	...	16.12 ± 0.04[b]	...	0.31 ± 0.05[b]	1994 Dec
4..........................	22.3 ± 0.2	1.3 ± 0.2	...	...	...	...	1994 Sep–1995 Jan
5..........................	22.35 ± 0.17	1.41 ± 0.20	...	...	...	...	1994 Sep–1995 Mar
6..........................	22.05 ± 0.10[c]	1.31 ± 0.12	2.26 ± 0.12	17.44 ± 0.09	0.95 ± 0.10	0.16 ± 0.16	2000/2001/2003

[a] Year and month the data were obtained.
[b] Data cannot be reconciled with 2MASS (see text).
[c] $B - V = 1.17 \pm 0.17$.

REFERENCES—(1) Zhao et al. 1994; (2) Casares et al. 1995; (3) Beekman et al. 1997; (4) Callanan et al. 1996; (5) Garcia et al. 1996; (6) this paper.

comparing red optical spectra of the SXT secondary star with various spectral types from the same luminosity class. Because of the orbital motion of J0422+32 (±372 km s^{-1}), the photospheric absorption lines are broadened by rotation. This effect is usually accounted for during the analysis of the spectral data. The optical spectrum may also suffer from contamination. Both effects can weaken the apparent line strengths and make stellar classification difficult. Another difficulty is that to classify the secondary star in these systems, it is assumed that the gravity and abundances of the secondary star are consistent with those of the main-sequence templates used to derive the spectral type. Given the low signal-to-noise ratio (S/N) of these data, deriving a spectral type can be challenging.

Alternatively, one can use a spectral energy distribution (SED) and the above limits on the spectral type to derive not only an effective temperature of the secondary star, but also estimates for both the visual extinction and contamination level. Although difficulties similar to finding the spectral type of the secondary star from spectra may be encountered when using broadband photometry, the effective temperature is less sensitive to changes in the gravity and abundances than the shape and depth of individual spectral features. Given the higher S/N, an effective temperature derived using photometry can be just as useful as a spectral type derived from the spectroscopic data set. We present the optical-infrared ($BVRIJHK$) SED for J0422+32 in Figure 3. In this figure we compare the observed SED to those for an M1 V and an M4 V (Bessell & Brett 1988; Bessell 1991; Mikami & Heck 1982). We find that after dereddening the observed data by $A_V = 0.74$ mag, the best-fitting spectral type is that of an M1 V. This extinction is consistent with published values. Shrader et al. (1994) calculate $E(B - V) = 0.2 \pm 0.1$ from the 5780 Å diffuse interstellar feature, $E(B - V) = 0.23 \pm 0.02$ from an optical continuum power-law fit, and finally, $E(B - V) = 0.40 \pm 0.06$ from an ultraviolet 2170 Å interstellar feature. Our color excess of $E(B - V) = 0.24 \pm 0.03$ from SED fitting is consistent with the optically derived excess from Shrader et al. (1994), as well as those from King, Harrison, & McNamara (1996), Callanan et al. (1995), and Martin et al. (1995). Based on the results from Figure 3, we adopt an extinction value of $A_V = 0.74 \pm 0.09$ mag, a secondary star spectral type of M1, and a corresponding temperature of $T_{\rm eff} = 3900$ K (Gray 1992).

An M1 V spectral type is consistent with those found by Casares et al. (1995) and Harlaftis et al. (1999), but not with the M4 V type arrived at by Webb et al. (2000). A spectral type of M4 V cannot be made consistent with the observations, no matter the extinction. The only way to make a spectral type as late as M4 work with the observations is to posit the existence of an additional source of blue luminosity in the system. However, as is clear from the SED, such a source would have to supply 70% of the flux in the R band and would dominate the red optical spectra. We address the issue of contamination in § 3.2.

It can be seen from Table 1 that the infrared data presented by Beekman et al. (1997) are not consistent with our photometry. While the optical magnitudes and colors have shown very little evidence for change since J0422+32 entered quiescence, the infrared luminosity of the source appears to have declined by more than a magnitude. By combining data from Casares et al. (1995) with that of Beekman et al. (1997), taken within the same month, we find that $V - K = 6.12$ in 1994. If we assume that $A_V = 0.74$, the dereddened value is $(V - K)_0 = 5.46$. This corresponds
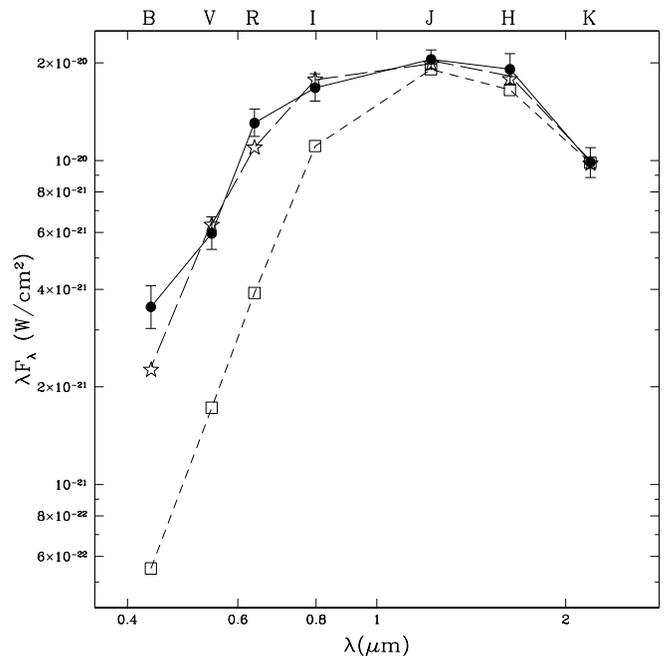

FIG. 3.—J0422+32 optical-infrared quiescent SED dereddened by $A_V = 0.74$ mag (*filled circles*). The infrared (*JHK*) points represent phase-averaged data. Error bars are 1 σ. These data are compared to the SED for an M1 V (*open stars*) and an M4 V (*open squares*), normalized at K. The M1 V SED fits that of J0422+32, with exceptions at B (34%) and R (8%).

to a spectral type of M4/5 V. Using the dereddened color from Casares et al. (1995), $(V - I)_0 = 1.72$, a spectral type of M0 V $\pm$ 1 is derived. These two colors are completely inconsistent: the $V - I$ color of an M4/5 V is 3.0 $\pm$ 0.2. This should be compared with our values of $(V - I)_0 = 1.96$ (M1 V) and $(V - K)_0 = 3.95$ (M1 V).

It seems difficult to understand this type of change. We have examined the 2MASS values for the secondary standards used by Beekman et al. (1997) and have been unable to reproduce their photometry. First, in the notes of their Table 2, they appear to have confused the identification of their two standard stars with those of Chevalier & Ilovaisky (1995). In Chevalier & Ilovaisky (1995) star No. 4 is the brighter of the two stars and must correspond to their "Standard-1" (although it is possible that star No. 4 is variable, no evidence to this effect is found in our long-term data). Even with the correct identification, however, their photometry does not agree with the 2MASS values. If there were simply a zero-point offset, the differences between the two sets of magnitudes would be consistent. We do not find any such consistency. We are unable to determine the source of this problem, but there does appear to be something unusual about the Beekman et al. (1997) infrared photometry that extends beyond a mere zero-point correction.

We conclude that the spectral type of the secondary star is M1 V$\pm$1, consistent with all of the previous assignments except that of Webb et al. (2000). While the methodology used by Webb et al. (2000) is robust for normal, late-type main-sequence stars, it is unclear whether the secondary stars in SXTs can be considered to be normal main-sequence stars. Again, broadband photometry is not as sensitive to changes in gravity and abundances as spectral features; however we do use main-sequence data in the SED and atmosphere models (see § 3.3). Therefore, for completeness we have run models in which the spectral type of the secondary star was assigned an effective temperature of an M4 V, the spectral type determined by Webb et al. (2000). We find that our result does not significantly change with this variation in spectral type.

3.2. Estimating the Amount of Infrared Nonstellar Light

If we assume a spectral type of M1 V and $A_V = 0.74$ mag, there is very little room in the $VRIJHK$ SED for contamination from other sources in the system. Because the level of contamination is an extremely important quantity, acting to dilute the ellipsoidal variations, we address the issue here. There have been a number of estimates for the level of the R-band contamination in the J0422+32 system, ranging from less than 20% (Callanan et al. 1996) to up to 60% (Casares et al. 1995; Filippenko et al. 1995). In our SED, we find that there is about an 8% excess in the R band that could be attributed to Hα emission. Estimating the level of contamination in an optical spectrum that has limited wavelength coverage is more difficult than determining the spectral type—it suffers from many of the same issues while attempting to fit a continuum to the observed spectrum.

It is clear from the SED that combinations of a hot and a cool source can reproduce the observed spectrum. Note, however, that whatever "hot" source (anything hotter than an M1 V) one selects so as to reproduce the $BVRI$ data by combining it with a very late type dwarf, it will have only minor effects in the infrared. No one has proposed a spectral type later than M4 for the secondary star. If one chooses an

M4 V spectral type for the companion and normalizes the SED to the observed K-band flux, then the secondary star only supplies 30% of the observed R-band flux. This fraction, of course, is even smaller if you do not normalize to the K-band flux. Thus, the level of contamination in the R-band using an M4 secondary star (70%) is larger than any of the existing estimates for this contamination. The optical spectrum of such a heavily contaminated source would be highly diluted and quite difficult to extract. As one adjusts the spectral type of the companion to earlier types, the dilution is lessened. An M2 V would have a dilution of 24% at R, with the star contributing 76% of the flux.

The most difficult contamination source to extract in the case of J0422+32 is the one that has the *shallowest spectral slope*. The most relevant emission process with the shallowest slope is free-free emission, which in λF_λ space has a spectrum proportional to λ^{-1}. If we ascribe the entire B-band excess (34%) to free-free emission, then in the K-band, the contamination would be ~7%. Such a low level of contamination would be difficult to detect, given the S/N of the current data. *Any other proposed process, such as synchrotron emission or classical accretion disk spectra, produces a steeper spectrum in λF_λ than free-free emission, and thus will dilute the infrared ellipsoidal variations by a smaller amount than free-free emission.*

A very conservative estimate of the disk contamination in the infrared is based on the assumption that the optically thin disk indeed radiates through free-free emission processes. A 7% contamination in the infrared bands would cause the observed orbital inclination angle of the system to be underestimated by $\leq 2°$.

3.3. Ellipsoidal Models

As in GHM01 and GHO01, we modeled the infrared light curves of J0422+32 with WD98 (Wilson 1998; see GHM01 for references and a basic description of the code, and Gelino 2001 for a more comprehensive description). We ran WD98 for a semidetached binary with the primary having such a large gravitational potential that it essentially has zero radius. The most important adopted wavelength-independent input values to WD98 are listed in Table 2, and the wavelength-dependent values are listed in Table 3.

The models were run for a range of inclination angles with parameters for an M0 V through an M4 V secondary star. The secondary star atmosphere was determined from solar-metallicity Kurucz models. The Kurucz atmosphere models are computed in temperature steps of 250 K for the range we are interested in, and stop at 3500 K. We therefore

TABLE 2
WAVELENGTH-INDEPENDENT WD98 INPUT PARAMETERS

Parameter	Value
Orbital period	0.2121600 days
Ephemeris (HJD phase 0.0)[a]	2450274.4156
Orbital eccentricity..	0.0
Temperature of secondary.................................	3900 K
Mass ratio (M_2/M_1).......................................	0.116
Atmosphere model..	Kurucz (log g = 4.59)
Limb-darkening law...	Square root
Secondary star gravity-darkening exponent	$\beta_1 = 0.27$
Secondary star bolometric albedo	0.676

[a] From Webb et al. 2000.

TABLE 3
WAVELENGTH-DEPENDENT WD98 INPUT PARAMETERS

Parameter	J	H	K
Square root limb-darkening coefficient x_λ	-0.137	-0.146	-0.160
Square root limb-darkening coefficient y_λ	0.718	0.655	0.592

TABLE 4
DERIVED PARAMETERS FOR J0422+32

Parameter	Value
Orbital inclination angle	$45° \pm 2°$
Primary object mass M_1	$3.97 \pm 0.95\ M_\odot$
Secondary star mass M_2	$0.46 \pm 0.31\ M_\odot$
Orbital separation a	$2.45 \pm 0.24\ R_\odot$
Secondary star radius R_{L_2}	$0.53 \pm 0.16\ R_\odot$
Adopted distance	2.49 ± 0.30 kpc

use extrapolated fluxes for the cooler parts of the star. For reasons cited above, we have used normal, nonirradiated, limb-darkening coefficients in the models (van Hamme 1993). We also adopted gravity-darkening exponents found by Claret (2000), and a mass ratio, q, of $0.116^{+0.079}_{-0.071}$ (Harlaftis et al. 1999). We ran models assuming the secondary star was the only source of *infrared* light in the system. We also assumed that the secondary star had a uniform surface brightness aside from limb- and gravity-darkening effects (i.e., no star spots).

The best-fit model was determined using χ^2 tests. We found that changing the spectral type of the secondary from an M4 V to an M0 V resulted in a change in the orbital inclination angle of $<1°$. Similarly, varying q from 0.045 to 0.195 affected i by $\leq 1°$. We find that the best-fitting J-, H-, and K_s-band model has $i = 45°$ and the parameters found in Table 2. Figure 2 presents this best-fitting model for the J-, H-, and K_s-band light curves.

3.4. *The Adopted Model and Its Uncertainties*

Assuming all of the infrared light in the system comes from the secondary star, the best-fitting orbital inclination angle for J0422+32 is $i = 45°$. If this assumption were incorrect and significant infrared contamination were present in the system, each light curve would most likely be diluted by a different amount, causing the best-fit inclination for each band to be different from the others. We find instead that all three infrared light curves give a consistent $45°$ best fit, whether solved simultaneously or individually.

If there is no contamination affecting the infrared light curves, the absolute lower limit to the inclination angle is $43°$. This corresponds to an upper limit to the compact object mass of $4.92\ M_\odot$, firmly placing it below $5\ M_\odot$. Using an estimate of 7% for the infrared accretion disk contamination in the system gives an inclination of $45^{+2.8}_{-2}$ degrees; however, we do not believe that the infrared light curves are significantly affected by any such contamination. Therefore, based on the error in q, the spectral type (i.e., temperature) of the secondary star, and the photometric error bars, the adopted orbital inclination angle is $45° \pm 2°$. Combining this inclination with the observed mass function, we find the mass of the primary object to be $3.97 \pm 0.95\ M_\odot$.

Using the mass of the compact object and the orbital period, the orbital separation of the two components in the system can be computed. This, in turn, can be combined with the mass ratio to find the size of the Roche lobe for the secondary star. The temperature of the secondary and its Roche lobe radius are then used to find the secondary's bolometric luminosity and bolometric absolute magnitude. After accounting for the bolometric correction (Bessell 1991), the distance modulus for the J, H, and K bands is

used to find an average distance of 2.49 ± 0.30 kpc. Table 4 lists all of the derived parameters for J0422+32.

4. DISCUSSION

In this paper, we have presented the first observed infrared ellipsoidal variations for J0422+32. The derived parameters in Table 4 are based on the modeling of these variations, assuming no significant contamination from any other sources of infrared light in the system. Even though there is a large range of published inclination angles for this system, the inclination angle found here is consistent with those found by Orosz & Bailyn (1995), $\geq 45°$; Filippenko et al. (1995), $45°–51°$; Callanan et al. (1996), $<45°$; and Webb et al. (2000), $\leq 45°$; and suggests that we should not be overly surprised that this system harbors a low-mass object.

Even though the errors determined here for the orbital inclination angle and mass of the primary object are smaller than previously published, the nature of the primary object in this system remains unclear. Both the optical and X-ray outburst light curves of J0422+32 closely resemble those of the prototype black hole SXT, V616 Mon. However, since its initial outburst, the system has exhibited a series of mini-outbursts similar to those observed from neutron star X-ray binaries such as Aql X-1 (Charles et al. 1980). Martin et al. (1995) not only compare this SXT with Aql X-1, but also compare J0422+32 to GX 339-4, an X-ray binary system thought to be a black hole candidate based on its rapid X-ray variability, and because it exhibits "high," "low," and "off" states (Markert et al. 1973). They conclude their study by saying, "J0422+32 would seem to be a system whose nature is intermediate between the X-ray transients and those which show more than one mode of accretion."

We find the minimum mass of the primary object to be just below the maximum accepted mass for a neutron star. However, just about all neutron stars with measured masses cluster around $1.35\ M_\odot$, with a small spread of $\pm 0.04\ M_\odot$ (van Kerwijk 2001). For the compact object in this system to have a mass consistent with that of a typical neutron star, the orbital inclination angle would have to be about $85°$, which is ruled out by a lack of eclipses during outburst. In addition, contamination at the 160% level in the infrared is needed to account for a $40°$ underestimation of the inclination angle. This level of contamination surely would be visible in the SED and rule out any possibility of detecting the secondary star in the optical. Therefore, until more compelling evidence for a neutron star primary is presented, we suggest that the primary object in J0422+32 is a low-mass black hole.

Recently, two papers (GHO01; Greiner, Cuby, & McCaughrean 2001) have published evidence for the

highest mass stellar black holes. Here we find what appears to be the lowest mass stellar black hole. A handful of other sources may be potential candidates, based on their observed mass functions, but current findings suggest otherwise. The most likely candidate to join J0422＋32 as a low-mass black hole is GRS 1009-45. The current estimates of the compact-object mass span from 4.64 to 5.84 $M_\odot$ (Gelino 2002), with a lower limit of 4.4 $M_\odot$ from lack of X-ray eclipses (Filippenko et al. 1999). Thus, we contend that J0422＋32 contains the lowest mass stellar black hole and is the first to have a measured mass that falls in the 3–5 $M_\odot$ range.

REFERENCES

Beekman G., Shahbaz, T., Naylor, T., Charles, P. A., Wagner, R., & Martini, P. 1997, MNRAS, 290, 303
Bessel, M. S. 1991, AJ, 101, 662
Bessell, M. S., & Brett, J. M. 1988, PASP, 100 1134
Bonnet-Bidaud, J., & Mouchet, M. 1995, A&A, 293, L69
Callanan, P. J., Garcia, M., Filippenko, A. V., McLean, I., & Teplitz, H. 1996, ApJ, 470, L57
Callanan, P. J., et al. 1995, ApJ, 441, 786
Casares, J., Martin, A., Charles, P. A., Martín, E., Rebolo, R., Harlaftis, E., & Castro-Tirado, A. 1995, MNRAS, 276, L35
Castro-Tirado, A. J., Pavlenko, E. P., Shlyapnikov, A. A., Brandt, S., Lund, N., & Ortiz, J. L. 1993, A&A, 276, L37
Charles, P. A. 2001, in Black Holes in Binaries and Galactic Nuclei, ed. L. Kaper, E. P. J. van den Heuvel, & P. A. Woudt (Berlin: Springer), 27
Charles, P. A., et al. 1980, ApJ, 237, 154
Chevalier, C., & Ilovaisky, S. 1995, A&A, 297, 103
———. 1996, A&A, 312, 105
Claret, A. 2000, A&A, 359, 289
Filippenko, A. V., Leonard, D. C., Matheson, T., Li, W., Moran, E. C., & Riess, A. G. 1999, PASP, 111, 969
Filippenko, A. V., Matheson, T., & Ho, L. 1995, ApJ, 455, 614
Garcia, M. R., Callanan, P. J., McClintock, J. E., & Zhao, P. 1996, ApJ, 460, 932
Gelino, D. M. 2001, Ph.D. thesis, New Mexico Sate Univ.
———. 2002, BAAS, 34, 654
Gelino, D. M., Harrison, T. E., & McNamara, B. J. 2001, AJ, 122, 971 (GHM01)

Gelino, D. M., Harrison, T. E., & Orosz, J. A. 2001, AJ, 122, 2668 (GHO01)
Gray, D. F. 1992, The Observations and Analysis of Stellar Photospheres (New York: Cambridge Univ. Press)
Greiner, J., Cuby, J. G., & McCaughrean, M. J. 2001, Nature, 414, 522
Harlaftis, E. T., Collier, S., Horne, K., & Filippenko, A. V. 1999, A&A, 341, 491
King, N. L., Harrison, T. E., & McNamara, B. J. 1996, AJ, 111, 1675
Markert, T. H., Canizares, C. R., Clark, G. W., Lewin, W. H. G., Schnopper, H., W., & Sprott, G. F. 1973, ApJ, 184, L67
Martin, A. C., Charles, P. A., Wagner, R. M., Casares, J., Henden, A. A., & Pavlenko, E. P. 1995, MNRAS, 274, 559
Mikami, T., & Heck, A. 1982, PASJ, 34, 529
Orosz, J. A., & Bailyn, C. D. 1995, ApJ, 446, L59
Paciesas W. S., & Briggs M. S. 1992, IAU Circ. 5580
Shrader, C. R., Wagner, R. M., Hjellming, R. M., Han, X. H., & Starrfield, S. G. 1994, ApJ, 434, 698
van Hamme, W. 1993, AJ, 106, 2096
van Kerkwijk, M. H. 2001, in Black Holes in Binaries and Galactic Nuclei, ed. L. Kaper, E. P. J. van den Heuvel, & P. A. Woudt (Berlin: Springer), 39
Webb, N. A., Naylor, T., Ioannou, Z., Charles, P. A., & Shahbaz, T. 2000, MNRAS, 317, 528
Wilson, R. E. 1998, Computing Binary Star Observables (Gainsville: Univ. of Florida)
Zhao, P., Callanan, P., Garcia, M., & McClintock, J. 1994, IAU Circ. 6072